Rydberg Series as Ionization Channels: Photoabsorption and Photoionization of the Atmospherically Relevant Molecule NO

E. Bustos, A. M. Velasco, I. Martín,* and C. Lavín

Departamento de Química Física, Facultad de Ciencias, Universidad de Valladolid, 47005 Valladolid, Spain

Received: November 25, 2002; In Final Form: June 4, 2003

The photoionization of nitric oxide from its ground state has been studied with the molecular-adapted quantum defect orbital (MQDO) method. Partial differential oscillator strengths for the different Rydberg series that constitute the ionization channels of NO from its ground state have been calculated up to a photon energy of 60 eV. The continuity of the calculated differential oscillator strengths across the ionization threshold, that is, in the discrete and continuous regions of the spectrum, has been adopted as a quality criterion, given the scarcity of comparative data.

I. Introduction

Molecular photoionization processes are of fundamental importance[1] and find application in a large number of scientific contexts, including aeronomy,[2] astrophysics[3], planetary sciences,[4] radiation chemistry, physics, and biology. Workers in these fields require reliable absolute cross sections for partial photoionization, and total photoabsorption and photoionization as well as for photofragmentation processes over wide spectral ranges, particularly for use in modeling studies.[5−7]

Although experimental studies of molecular total photoabsorption and total photoionization cross sections in the vacuum ultraviolet (VUV) and soft X-ray regions have experienced steady progress since the early 1950s, quantitatively reliable absolute partial photoionization and photofragmentation cross sections have been achieved only recently[8] with techniques such as those based on synchroton radiation, where the spectral variation of the cross sections and angular distributions can be studied over a wide continuous range of incident photon energy.[9] Another widely employed experimental approach is low-resolution dipole (e, e) spectroscopy that uses fast electrons[10−12] as a virtual photon source. It should be noted that these real- and virtual-photon experiments are complementary to each other when it comes to understanding the essential features of the interaction of VUV photons with molecules.[13]

Theoretical calculations of partial photoionization cross sections at reliable levels of approximation have also appeared relatively recently with the advent of refined computational techniques and the increasing availability of large, high-speed computers.[8] However, given the growing interest in molecular photoionization processes, particularly in the specific partial channels that contribute to the overall photoabsorption, many experimentalists demand new and reliable theoretical calculations that may help in the assignment of the measurements.

In this work, we have focused our attention on nitric oxide because we find its study both timely and relevant for several reasons. It plays an essential role in the physics and chemistry of the earth's upper atmosphere[14] and is closely related to pollution problems. The dissociative recombination processes[15] of NO, where Rydberg states are directly involved, are relevant, for example, in the E and F regions of the ionosphere.[15] Here, NO^+ is one of the most abundant molecular ions, and the hot oxygen thus produced in the photodissociation of NO contributes to the maintenance of the nighttime ionosphere.[16] In addition to their intrinsic spectroscopic interest, the quantitative aspects of the interaction of NO with UV and soft X-ray radiation are of practical importance in several other contexts. Furthermore, the fact that the ground state of NO exhibits an open-shell electron configuration with symmetry other than Σ, represents a formidable challenge to theorists in the accurate calculation of partial photoionization oscillator strengths.[17] In the present paper, we report theoretical absorption oscillator strengths in both the discrete and continuous regions of the spectrum for a number of Rydberg series that serve as partial ionization channels for this molecule. The molecularly adapted quantum defect orbital (MQDO) methodology, which has supplied reliable intensities for Rydberg transitions in a variety of molecular species[18−21] and accurate molecular photoionization cross sections,[22,23] has been employed. The correctness of the present results for NO has been assessed with the help of the scarce experimental and theoretical data available in the literature and by the criterion of continuity of the differential oscillator strengths across the ionization threshold for all of the Rydberg series (ionization channels) considered.

NO has a fairly complex photoelectron spectrum; furthermore, the energy levels of NO^+ are not directly accessible to conventional absorption spectroscopy. Very little information has been supplied by emission spectroscopy. The manifold of NO^+ states serve as convergence limits for an extensive set of Rydberg series of NO, which may autoionize or dissociate in various possible ways, yielding NO^+ ions or the fragments N^+ and $O^{\pm}$.[24] This gives rise to severe experimental difficulties mainly because of the large number of low-lying electronic states with various overlapping vibrational progressions.[25] The sparsity[9,17,26−28] of information on the energy dependence of the excitation cross sections of NO may be explained on the grounds of the complexity of the measurements, as mentioned above.

In earlier work, we illustrated the usefulness of analyzing the complete oscillator strength distribution in the discrete and continuous spectral regions for atoms.[29] In addition, the examination of this distribution over the entire spectral range

* Corresponding author. E-mail: imartin@qf.uva.es. Tel: +34-983-423272. Fax: +34-983-423013.

10.1021/jp022478q CCC: $27.50
Published on Web 02/21/2004

provides an excellent opportunity for finding useful items for further research, such as missing gaps in experimental data or the influence of autoionization processes or valence resonances originating in series mixing.

Additional goals of this work are to continue our recent studies of molecular systems with the MQDO approach[18−23] and to provide new and what we hope will be reliable and useful values of the photoionization cross sections corresponding to the excitation of a 2π electron from the electronic ground state of NO along the allowed Rydberg series. In section II, we present a brief outline of the computational method. In section III, the calculated spectral densities in the discrete and continuum regions are given and compared with available experimental and theoretical results.

In 1964, Mulliken[30] studied the influence of nuclear motions on molecular electronic structure. The presently reported intensities (in the form of absorption oscillator strengths) refer to vertical electronic transitions, which closely correspond to sums over vibrationally resolved cross sections constructed with the use of available Franck−Condon factors.[31] The latter can be directly compared with measurements that achieve vibrational resolution.[26,27]

II. Method of Calculation

The MQDO technique, formulated to deal with molecular Rydberg transitions, has been described in detail elsewhere.[18] A brief summary of this method follows. The MQDO radial wave functions are the analytical solutions of a one-electron Schrödinger equation that contains a model potential of the form

$$V(r)_a = \frac{(c - \delta_a)(2l + c - \delta_a + 1)}{2r^2} - \frac{1}{r} \qquad (1)$$

where a represents the set of quantum numbers that define a given molecular state. Solutions of this equation are related to Kummer functions. The parameter δ_a is the quantum defect, which is strongly dependent on the electron's angular momentum, and c is an integer chosen to ensure the normalization of the orbitals and their correct nodal pattern. For molecular systems, the noninfinite symmetry is accounted for by the angular part of the orbitals and consists of the appropriate linear combinations of spherical harmonics that form the bases for the irreducible representations of the molecule's symmetry group, to which a specific electronic state belongs. The quantum defect, δ_a, is related to the energy eigenvalue of the corresponding state through the following equation,

$$E_a = T - \frac{1}{2(n_a - \delta_a)^2} \qquad (2)$$

where T is the ionization energy. Both T and E_a are expressed here in hartrees.

The absorption oscillator strength for a transition between two bound states a and b may be expressed as

$$f(a \rightarrow b) = \frac{2}{3}(E_b - E_a)\, Q\{a \rightarrow b\}\, |R_{ab}|^2 \qquad (3)$$

The photoionization cross section for transitions between a bound a and a continuous state b is expressed as follows:

$$\sigma = \frac{4\pi^2 \alpha a_0^2}{3}\left[\frac{Z_{\text{net}}}{(n_a - \delta_a)^2} + k^2\right]\frac{1}{2k} Q\{a \rightarrow b\}\, |R_{ab}|^2 \qquad (4)$$

$k = (2E)^{1/2}$ is expressed in Rydberg atomic units, α is the fine-structure constant in au, and a_0 is the first Bohr radius. In eqs 3 and 4, the $Q\{a \rightarrow b\}$ are the nondimensional angular factors resulting from the integration of the factorized angular part of the transition moment, and R_{ab} is the radial contribution to the latter, expressed in atomic units.

The present calculations for both bound−bound and bound−continuum transitions have all been considered to take place through the electric dipole (E1) mechanism because this leads to the strongest bands. For both bound−bound and bound−continuum transitions, the radial transition moments result, within this model, in closed-form analytical expressions. We find this feature of our method to be one of its major advantages because it allows the calculation of intensity data free from the convergence problems that often plague some self-consistent-field procedures. The detailed algebraic expressions for the radial transition moments are given in ref 32 as originally formulated for photoionization in atomic systems and in ref 18 as generalized for bound−bound transitions in molecules.

III. Results and Analysis

The ground-state electronic configuration of NO possesses the following open-shell structure:

$$...(4\sigma)^2(1\pi)^4(5\sigma)^2(2\pi)^1 X^2\Pi$$

The ionization energy (IP) adopted in the present calculations was measured with the ZEKE technique by Sander et al.[33] ($74719.0 \pm 0.5\ \text{cm}^{-1}$). The experimental energy data employed for the $\ell = 0$, 1, and 2 bound Rydberg states are those compiled by Brunger et al.[28] For the $\ell = 3$ Rydberg states, we have used the theoretical values obtained with an R-matrix procedure by Rabadán and Tennyson.[34] The quantum defects for the different continua have been found through Edlèn[35] plots. That is, the δ value that corresponds to the bound states of a given Rydberg series is plotted against $(1/n^{*2})$, with n^* being the effective quantum number. Linear behavior is found unless the Rydberg series is subject to perturbations such as mixing with a valence state or with another Rydberg series. The series limit will be reached at $n = \infty$, that is, $(1/n^{*2}) = 0$. In Tables 1−4, we have collected the energy values and quantum defects employed in the present work.

We have recently reported in a study of the vibronic transitions of NO[36] that the above outermost molecular orbital (MO) closely resembles a "united atom" $3d\pi$ orbital of reduced size, with a smaller $2p\pi$ contribution, because of the asymmetry of the molecule.[37] Jungen[37] estimated the value of the overlap integral, S, between the $\Phi(2p\pi)$ non-Rydberg wave function and the $\Phi(3d\pi)$ "hydrogenic" function to be equal to 0.107. Then, the orthogonalized orbital could be expressed in the form

$$\Phi = (1 - S^2)^{-1/2}[\Phi^*(3d\pi) - S\Phi(2p\pi)]$$

Two constants were defined as

$$C_{3d\pi} = \frac{1}{[1 - S^2]^{1/2}}$$

and

$$C_{2p\pi} = -\frac{S}{[1 - S^2]^{1/2}}$$

such that the singly occupied MO in the ground-state configuration of NO may be denoted as $C_{3d\pi}\Phi^*(3d\pi) + C_{2p\pi}\Phi(2p\pi)$.

TABLE 1: Energies and Quantum Defects for Bound and Continuum $\ell = 0$ States of NO

state	E^a/cm^{-1}	δ
3sσ($A^2\Sigma^+$)	44231	1.103
4sσ($E^2\Sigma^+$)	60 863.80	1.1860
5sσ($S^2\Sigma^+$)	67 136	1.1965
6sσ($T^2\Sigma^+$)	69 961	1.1988
7sσ($Z^2\Sigma^+$)	71 460	1.1995
∞sσ	continuum	1.202

[a] Brunger et al.[28]

TABLE 2: Energies and Quantum Defects for Bound and Continuum $\ell = 1$ States of NO

state	E^a/cm^{-1}	δ
3pσ($D^2\Sigma^+$)	53 369	0.7329
4pσ($M^2\Sigma^+$)	64 660	0.6975
5pσ($R^2\Sigma^+$)	68 830	0.6842
6pσ($Y^2\Sigma^+$)	70 847	0.6781
∞pσ	continuum	0.6658
3pπ($C^2\Pi$)	52 418	0.7819
4pπ($K^2\Pi$)	64 336	0.7494
5pπ($Q^2\Pi$)	68 674	0.7402
6pπ($W^2\Pi$)	70 747	0.7455
∞pπ	continuum	0.7306

[a] Brunger et al.[28]

TABLE 3: Energies and Quantum Defects for Bound and Continuum $\ell = 2$ States of NO

state	E^a/cm^{-1}	δ
3dσ($H^2\Sigma^+$)	62 694.4	−0.0206
4dσ($O^2\Sigma^+$)	67 992.50	−0.0383
∞dσ	continuum	−0.0592
3dπ($H'^2\Pi$)	62 694.40	−0.0206
4dπ($O'^2\Pi$)	67 992.50	−0.0383
∞dπ	continuum	−0.0592
3dδ($F^2\Delta$)	62 043.34	0.0580
4dδ($N^2\Delta$)	67 609.09	0.0721
5dδ($U^2\Delta$)	70 210	0.0681
∞dδ	continuum	0.0778

[a] Brunger et al.[28]

Given the one-electron nature of the Rydberg states of NO (as widely accepted for all molecular Rydberg states), the Laporte selection rule $\Delta\ell = \pm 1$ has been applied to determine the electronically allowed transitions that may take place in the molecule, together with symmetry restrictions. Hence, we have focused our attention on the following transitions, all arising from the outermost MO of the molecular ground state: $X^2\Pi \rightarrow n\mathrm{s}\sigma'$, $n\mathrm{d}\sigma'$, $n\mathrm{d}\pi$, $n\mathrm{d}\delta$, and $X^2\Pi \rightarrow n\mathrm{p}\sigma$, $n\mathrm{p}\pi$, $n\mathrm{f}\sigma$, $n\mathrm{f}\pi$, $n\mathrm{f}\delta$.

The nature of the $n\mathrm{s}\sigma$ and $n\mathrm{d}\sigma$ Rydberg MOs also deserves a few remarks. Previous studies[37−39] agree with the idea that because the field inside the core is nonspherical it can mix up Rydberg orbitals that belong to the same irreducible representation within the $C_{\infty v}$ symmetry group but have different quantum numbers n and ℓ. It turns out that the $n\mathrm{d}\sigma$ orbitals of NO are strongly mixed with $(n+1)\mathrm{s}\sigma$[38] orbitals. The rotational structure of the $n\mathrm{d}\sigma$ Rydberg states, as observed by Huber and Miescher,[40] gives evidence that the $n\mathrm{d}\sigma$ MOs contain a large contribution of others with $\ell < 2$. Huber and Miescher[40] and, independently, Suter[41] carried out an early analysis of the ℓ uncoupling in this molecule, all concluding that the $n\mathrm{s}\sigma$ and $n\mathrm{d}\sigma$ Rydberg orbitals are actually mixtures of hydrogenic nd and $\ell < 2$ orbitals. Apparently, the origin of this mixing is the orthogonality constraint of the σ_g Rydberg orbitals to the σ core orbital, which is itself of mixed nature. Of the possible interaction partners, only states associated with $n\mathrm{s}\sigma$ MOs need be considered,

TABLE 4: Energies and Quantum Defects for Bound and Continuum $\ell = 3$ States of NO

state	E^a/cm^{-1}	δ
4fσ	67 835	0.0074
5fσ	70 314	0.0086
6fσ	71 661	0.0093
7fσ	72 473	0.0098
8fσ	73 000	0.0101
9fσ	73 361	0.0103
10fσ	73 619	0.0105
11fσ	73 810	0.0106
∞fσ	continuum	0.0110
4fπ	67 842	0.0054
5fπ	70 319	0.0059
6fπ	71 664	0.0063
7fπ	72 475	0.0066
8fπ	73 002	0.0067
9fπ	73 362	0.0068
10fπ	73 620	0.0069
11fπ	73 811	0.0071
∞fπ	continuum	0.0072
4fδ	67 857	0.0010
5fδ	70 327	0.0013
6fδ	71 669	0.0014
7fδ	72 478	0.0016
8fδ	73 004	0.0017
9fδ	73 364	0.0017
10fδ	73 621	0.0018
11fδ	73 812	0.0018
∞fδ	continuum	0.0019

[a] Rabadán and Tennyson.[34]

whereas those associated with n$p\sigma$ and n$p\pi$ orbitals can be ruled out for the following reasons:

(a) Couplings. The ℓ uncoupling in the np orbitals, observed by Dressler and Miescher[42] as a small Λ-type doubling, does not indicate any mixture with nd states.

(b) Symmetry. In the nearly nonpolar molecule NO, the p−d interaction is weaker than that of the s−d type. This result is to be expected because the atomic np orbitals have "u" inversion symmetry but both the ns and nd orbitals have "g" symmetry.

(c) Energy. The relative energy positions of p and d orbitals are such that p−d interactions are not favored. For each n value, the np state lies roughly midway between the nd and $(n-1)$d members of the same Rydberg series. However, the situation for the ns states is just the opposite: Only the low 3sσ state is far enough removed from any of the nd states to be considered independent.

Thus, for each n value, an isolated pair of quasi-degenerate Rydberg $^2\Sigma^+$ states is formed as follows: $|n\mathrm{d}\sigma'\rangle = C_1|(n+1)\mathrm{s}\sigma\rangle + C_2|n\mathrm{d}\sigma\rangle$ and $|(n+1)\mathrm{s}\sigma'\rangle = C_2|(n+1)\mathrm{s}\sigma\rangle - C_1|n\mathrm{d}\sigma\rangle$ with $C_1^2 + C_2^2 = 1$. Jungen[37] observed that both coefficients remained nearly constant along the Rydberg series and also commented on the need for mixing coefficients if we want to retain integral values for the quantum numbers n and ℓ in the characterization of molecular Rydberg series. Given the accuracy of Jungen's calculations,[37] we have presently adopted his values for C_1 and C_2, which are, respectively, −0.68 and 0.73 for the mixing of the $(n+1)\mathrm{s}\sigma - n\mathrm{d}\sigma$ ($n \geq 4$) Rydberg series and −0.64 and 0.77 to account for the $(n+1)\mathrm{s}\sigma - n\mathrm{d}\sigma$ ($n = 3$) mixing.

In Figures 1−4, we have graphically represented the MQDO oscillator strength spectral density in both bound and continuum spectral regions for the $X^2\Pi \rightarrow n\mathrm{s}\sigma'(\Sigma^+)$, $X^2\Pi \rightarrow n\mathrm{d}\sigma'(\Sigma^+)$, $X^2\Pi \rightarrow n\mathrm{p}\sigma(\Sigma^+)$, and $X^2\Pi \rightarrow n\mathrm{f}\sigma(\Sigma^+)$ absorption channels of NO. The oscillator strength spectral density, df/dE, in the continuum and the related oscillator strengths, f, in the discrete spectrum have been plotted in the same graph. We have

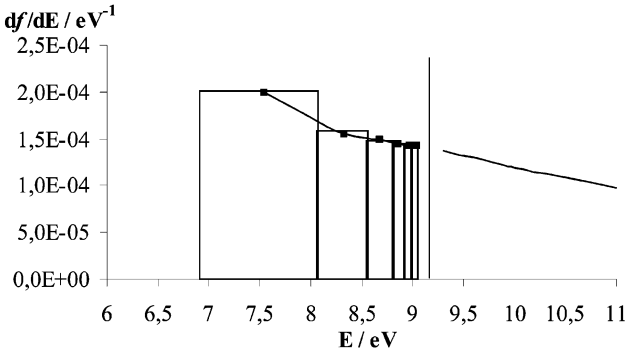

Figure 1. MQDO oscillator strength spectral density for the bound and continuum spectral regions of the $X^2\Pi \rightarrow ns\sigma'(\Sigma^+)$ ($n = 4-9, \infty$) Rydberg series in NO.

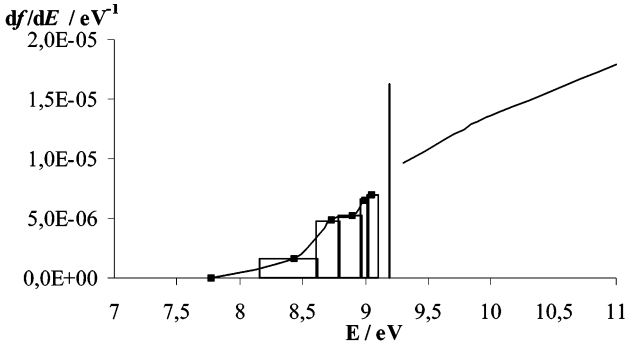

Figure 2. MQDO oscillator strength spectral density for the bound and continuum spectral regions of the $X^2\Pi \rightarrow nd\sigma'(\Sigma^+)$ ($n = 3-8, \infty$) Rydberg series in NO.

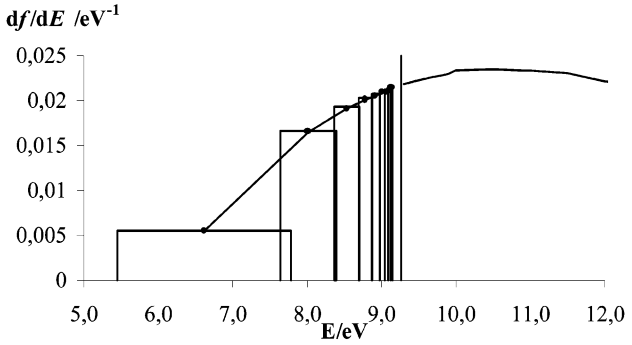

Figure 3. MQDO oscillator strength spectral density for the bound and continuum spectral regions of the $X^2\Pi \rightarrow np\sigma(\Sigma^+)$ ($n = 3-11, \infty$) Rydberg series in NO.

followed a procedure originally developed by Fano and Cooper[43] and later applied by other authors[44,45] as well as in some of our calculations on atomic and molecular systems.[22,23,29] The oscillator strengths of the discrete transitions are included in the plot in the form of a histogram. The continuum is included in terms of the spectral density of the oscillator strength, which is related to the photoionization cross section through the expression

$$\sigma(E) = 1.098 \times 10^{-16}\,\mathrm{cm}^2 \cdot \mathrm{eV}\left(\frac{\mathrm{d}f}{\mathrm{d}E/\mathrm{eV}}\right) \qquad (5)$$

The tops of the blocks in the histogram constructed in this way form a staircase, which should join smoothly with the d*f*/d*E* curve in the continuum across the ionization limit if the data are correct because the discrete part of the spectrum for any spectral series can be regarded as an appendage of the continuum.[43] An inspection of Figures 1−4 reveals complete

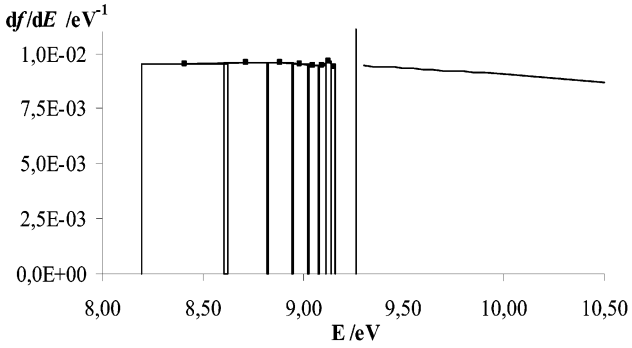

Figure 4. MQDO oscillator strength spectral density for the bound and continuum spectral regions of the $X^2\Pi \rightarrow nf\sigma(\Sigma^+)$ ($n = 4-11, \infty$) Rydberg series in NO.

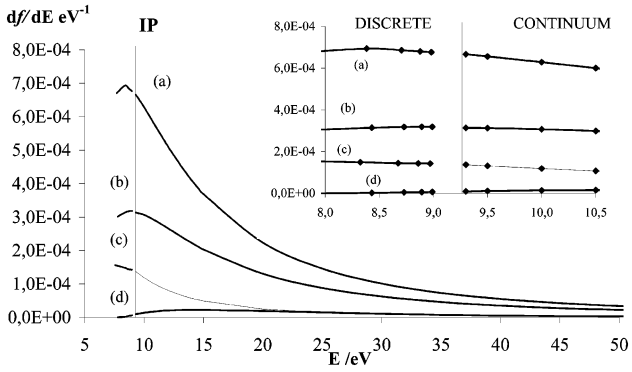

Figure 5. MQDO oscillator strength spectral density for the different Rydberg series of NO that arise from the excitation of the outermost electron in the ground state: (a) $X^2\Pi \rightarrow nd\delta(\Delta)$, (b) $X^2\Pi \rightarrow nd\pi(\Pi)$, (c) $X^2\Pi \rightarrow ns\sigma'(\Sigma^+)$, (d) $X^2\Pi \rightarrow nd\sigma'(\Sigma^+)$. (Inset) Enlarged spectral region around the ionization threshold.

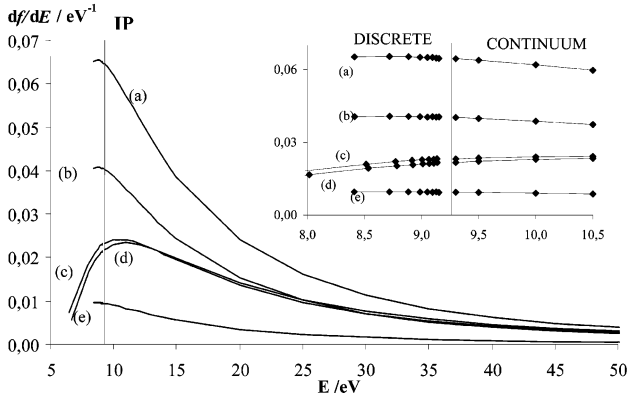

Figure 6. MQDO oscillator strength spectral density for the different Rydberg series of NO that arise from the excitation of the outermost electron in the ground state: (a) $X^2\Pi \rightarrow nf\pi(\Pi)$, (b) $X^2\Pi \rightarrow nf\delta(\Delta)$, (c) $X^2\Pi \rightarrow np\pi(\Pi)$, (d) $X^2\Pi \rightarrow np\sigma(\Sigma^+)$, (e) $X^2\Pi \rightarrow nf\sigma(\Sigma^+)$. (Inset) Enlarged spectral region around the ionization threshold.

consistency between the MQDO photoionization cross sections and oscillator strengths, in the sense just described, for all the Rydberg series studied. In the absence of comparative experimental values, these features make us feel confident in the (at least qualitative) reliability of the present MQDO data. An additional reason for our confidence in the present results is the very good accord found between MQDO oscillator strengths, which were recently reported for the first few members of the *n*s and *n*p Rydberg series of NO[36] with the experimental data available in the literature.

In Figures 5 and 6, we have depicted the MQDO d*f*/d*E* values versus the incident photon energy for the Rydberg series to

TABLE 5: Photoionization Cross Sections (in Mb) Leading to the $(2\pi)^{-1}$ $X^1\Sigma^+$ State of NO^+ as a Function of the Incident Photon Energy (in eV)

E/eV	MQDO[a]	exptl[b]	exptl[c]	theor[d]	theor[e]
17.0	10.04		8.4 ± 0.8	3.71	3.76
18.0	9.19		4.4 ± 0.2	3.73	3.80
19.0	8.46	8.11		3.71	3.83
20.0	7.79	6.97	3.2 ± 0.1	3.79	3.81
21.0	7.20	5.16		3.82	3.78
22.0	6.66	5.27	3.7 ± 0.1	3.93	3.75
23.0	6.19		4.1 ± 0.1	4.05	3.72
24.0	5.73	5.34		4.04	3.65
25.0	5.34		4.6 ± 0.1	4.04	3.56
26.0	4.98	6.04	4.9 ± 0.1	3.96	3.43
27.0	4.65		5.0 ± 0.2	3.87	3.35
28.0	4.35	6.08	5.1 ± 0.2	3.71	3.26
30.0	3.83	5.42	5.0 ± 0.2	3.55	3.06
32.0	3.40	5.02		3.44	2.87
34.0	3.04	4.29		3.16	2.68
36.0	2.69	3.76		2.89	2.48
38.0	2.42	3.46		2.51	2.27
40.0	2.19	2.91		2.18	2.11
42.0	1.99	2.56			1.98
44.0	1.81	2.35			1.86
46.0	1.65	2.13			1.71
48.0	1.53	1.92			1.58
50.0	1.40	1.69			1.47
52.0	1.30	1.56			1.36
54.0	1.20	1.55			1.27
56.0	1.11	1.36			
58.0	1.02	1.08			
60.0	0.95	1.06			

[a] MQDO, this work. [b] Iida et al.[26] [c] Southworth et al.[27] [d] Smith et al.[9] [e] Hermann et al.[17]

which the excitation of the ground state's $X^2\Pi$ outermost electron gives rise. The energy covered the range from 5−60 eV. These Rydberg series constitute different possible photoionization channels from the ground state of NO. Our main purpose has been to show the expected monotonic decrease with increasing free-electron energy exhibited by almost all of these spectral series in the continuum, given that these series are not expected to suffer from perturbations such as autoionization. This regular behavior may also allow a safe extrapolation of the spectral density at higher energies than reported, if needed (e.g., in designing future experiments). In Figure 5, the anomalous behavior of the $ns\sigma'$ Rydberg series, created by its mixing with the $nd\sigma'$ series, is also reproduced. The latter Rydberg series also deviates from a hydrogenic trend, even though it is not so clearly apparent in the Figure.

Finally, in Table 5 we collect cross-section values leading to the $(2\pi)^{-1}$ $X^1\Sigma^+$ state of NO^+ within an energy range of 17−60 eV. The MQDO total cross section at different photon energies has been determined by adding the contributions of the compatible channels, *j*:

$$\sigma_i(h\nu) = \sum_j \sigma_{i\rightarrow j}(h\nu) \qquad (6)$$

That is, we have obtained the total cross section for the ionization of NO from its ground state, $X^2\Pi$, through the nine compatible ionization channels found: $X^2\Pi \rightarrow ns\sigma'(\Sigma^+)$, $X^2\Pi \rightarrow nd\sigma'(\Sigma^+)$, $X^2\Pi \rightarrow nd\pi(\Pi)$, $X^2\Pi \rightarrow nd\delta(\Delta)$, $X^2\Pi \rightarrow np\sigma(\Sigma^+)$, $X^2\Pi \rightarrow np\pi(\Pi)$, $X^2\Pi \rightarrow nf\sigma(\Sigma^+)$, $X^2\Pi \rightarrow nf\pi(\Pi)$, and $X^2\Pi \rightarrow nf\delta(\Pi)$. The numerical values of the partial cross sections are collected in Tables 6 and 7. In Table 5, we have also included the experimental measurements by Iida et al.[26] and Southworth et al.[27] as well as some theoretical values available in the literature.[9,17] Iida et al.[26] employed dipole (e, 2e) spectroscopy over a wide range of equivalent photon energy. Southworth et al.[27] measured photoionization cross sections for the valence molecular orbitals of NO over the range of 16−31 eV with synchrotron radiation. However, the different proce-

TABLE 6: Photoionization Cross Sections (in Mb) for the Different Rydberg Channels Arising from the Excitation of the Outermost Electron in the Ground State, $X^2\Pi$, of NO

E/eV	$X^2\Pi \rightarrow$ $\infty s\sigma'(\Sigma^+)$	$X^2\Pi \rightarrow$ $\infty d\sigma'(\Sigma^+)$	$X^2\Pi \rightarrow$ $\infty d\pi(\Pi)$	$X^2\Pi \rightarrow$ $\infty d\delta(\Delta)$
17.0	0.00399	0.00237	0.0186	0.0328
18.0	0.00349	0.00229	0.0170	0.0296
19.0	0.00306	0.00220	0.0156	0.0269
20.0	0.00271	0.00211	0.0143	0.0245
21.0	0.00240	0.00201	0.0132	0.0224
22.0	0.00215	0.00192	0.0121	0.0205
23.0	0.00193	0.00182	0.0112	0.0188
24.0	0.00173	0.00174	0.0104	0.0173
25.0	0.00157	0.00165	0.0097	0.0160
26.0	0.00145	0.00153	0.0090	0.0148
27.0	0.00130	0.00149	0.0084	0.0137
28.0	0.00123	0.00135	0.0078	0.0127
29.0	0.00116	0.00128	0.0073	0.0119
31.0	0.00105	0.00106	0.0064	0.0103
32.0	0.00095	0.00097	0.0060	0.0097
34.0	0.00088	0.00089	0.0054	0.0085
36.0	0.00082	0.00084	0.0048	0.0076
38.0	0.00076	0.00078	0.0043	0.0067
40.0	0.00071	0.00058	0.0039	0.0060
42.0	0.00065	0.00049	0.0035	0.0054
44.0	0.00060	0.00044	0.0032	0.0049
46.0	0.00057	0.00040	0.0029	0.0045
48.0	0.00052	0.00037	0.0027	0.0041
50.0	0.00049	0.00033	0.0024	0.0037
52.0	0.00043	0.00028	0.0022	0.0034
54.0	0.00042	0.00027	0.0021	0.0031
56.0	0.00040	0.00025	0.0019	0.0029
58.0	0.00037	0.00024	0.0018	0.0027
60.0	0.00035	0.00021	0.0016	0.0025

TABLE 7: Photoionization Cross Sections (in Mb) for the Different Rydberg Channels Arising from the Excitation of the Outermost Electron in the Ground State, $X^2\Pi$, of NO

E/eV	$X^2\Pi \rightarrow$ $\infty p\sigma(\Sigma^+)$	$X^2\Pi \rightarrow$ $\infty p\pi(\Pi)$	$X^2\Pi \rightarrow$ $\infty f\sigma(\Sigma^+)$	$X^2\Pi \rightarrow$ $\infty f\pi(\Pi)$	$X^2 \rightarrow$ $\infty f\delta(\Delta)$
17.0	1.91	1.85	0.51	3.49	2.19
18.0	1.78	1.72	0.46	3.18	2.00
19.0	1.67	1.60	0.42	2.90	1.82
20.0	1.56	1.49	0.38	2.65	1.67
21.0	1.46	1.39	0.35	2.43	1.53
22.0	1.36	1.30	0.32	2.23	1.41
23.0	1.28	1.21	0.30	2.06	1.30
24.0	1.20	1.13	0.27	1.90	1.20
25.0	1.13	1.06	0.25	1.76	1.11
26.0	1.06	0.99	0.24	1.63	1.03
27.0	1.00	0.93	0.22	1.52	0.96
28.0	0.94	0.88	0.20	1.42	0.89
29.0	0.89	0.83	0.19	1.32	0.83
31.0	0.79	0.74	0.17	1.16	0.73
32.0	0.75	0.70	0.16	1.09	0.68
34.0	0.68	0.63	0.14	0.96	0.61
36.0	0.61	0.56	0.12	0.85	0.54
38.0	0.55	0.51	0.11	0.76	0.48
40.0	0.50	0.46	0.10	0.69	0.43
42.0	0.46	0.42	0.09	0.62	0.39
44.0	0.42	0.39	0.08	0.56	0.35
46.0	0.39	0.35	0.07	0.51	0.32
48.0	0.36	0.33	0.07	0.47	0.29
50.0	0.33	0.30	0.06	0.43	0.27
52.0	0.31	0.28	0.06	0.39	0.25
54.0	0.29	0.26	0.05	0.36	0.23
56.0	0.27	0.24	0.05	0.33	0.21
58.0	0.25	0.22	0.04	0.31	0.19
60.0	0.23	0.21	0.04	0.29	0.18

dures applied to normalize the measured data in the two experiments[26,27] may have given rise to slight discrepancies between them, which would add to the ones inherent to the different measuring devices. As to the theoretical cross sections, these comprise the ones calculated with a static-exchange approximation procedure by Hermann et al.[17] and those obtained by the direct solution of the $e + NO^+$ equations at the static-exchange level by Smith and co-workers.[9] All of the authors pointed out the need for more accurate calculations in view of the complexity of the spectrum, the apparent absence of unambiguous assignments of higher-lying dipole excitation series, and the discrepancies among experimentally and theoretically determined cross sections.

The two sets of experimental cross sections,[26,27] if differing immediately after the ionization limit, that is, between 18 and 25 eV, display a minimum in the vicinity of 21 eV. The structure of the synchrotron radiation data[27] in the 15−20 eV range may presumably be attributed to the effect of autoionization. The MQDO cross sections conform fairly well to the more recent (e, 2e) experimental measurements[26] in the difficult region between about 19 and 24 eV to then reach good accord with both the synchrotron data[27] and the theoretical values of Smith et al.[9] up to 40 eV, the last incident photon energy at which these authors report their calculations. From 42 to 60 eV, good agreement is observed between the present results and the cross sections supplied by Hermann et al.[17] as well as the same decreasing trend as that of the (e, 2e) measurements.[26] No significant discrepancies among the existing data at higher photon energies are observed.

Nevertheless, Table 5 reveals the difficulties encountered by different experimental and theoretical procedures in yielding coincident data, particularly in the regions where the spectrum becomes complex. Despite the partial coincidences in some of the theoretical calculations and some of the observations, with the performance of the MQDO approach being rather satisfactory, the need for more refined calculations that may account for autoionization, for example, is suggested.

IV. Concluding Remarks

Partial and total photoionization cross sections of NO leading to the $(2\pi)^{-1}\ X^1\Sigma^+$ state of NO^+ have been calculated with the MQDO approach. Special remarks have been made with regard to the definitions of the 2π orbital and the $ns\sigma$ and $nd\sigma$ Rydberg states.

The present calculations constitute, in our view, a useful approximation to the spectrum. The reported excitation series of NO from its ground state, below the first ionization limit, are all confirmed to be Rydberg in nature, which is in good accord with the experimental findings. It may be of interest to notice that many of the cross-section values are large, suggesting potential autoionization features in high-resolution measurements; we intend to perform more refined studies of these features. Nonetheless, the continuity of the differential oscillator strength across the ionization threshold ensures that the results for the individual ionization channels are, at least, of qualitative correctness.

Even though the lack of very good agreement between the experimental and theoretical data from different sources over the entire energy range (5−60 eV) that was analyzed makes the difficulties in dealing with the photoionization of NO from its open-shell ground state apparent, the MQDO total photoionization cross sections are found to be in reasonable accord with the corresponding syhchroton-radiation and dipole (e, 2e) measurements and are in better agreement with the most recent experimental values of Iida et al.[26] than theoretical procedures based on static exchange techniques. We believe in the potential of the MQDO method for yielding good estimates in photoabsorption studies. Its analytical nature is one of its main attractive features.

Acknowledgment. This work has been supported by the D. G. I. of the Spanish Ministry for Science and Technology within project no. BQU2001-2935-C02, the European FEDER funds, and the J. C. L. within project VA 119/02. A.M.V. and E.B. also acknowledge their respective research contract and grant from the same institution and the Spanish Ministry for Education, Culture and Sports.

References and Notes

(1) Berkowitz, J. *Photoabsorption, Photoionization, Photoelectron Spectroscopy*; Academic: New York, 1979.
(2) Heicklein, J. A*tmospheric Chemistry*; Academic: New York, 1976.
(3) Spitzer, L., Jr. *Physical Processes in the Interstellar Medium*; Wiley: New York, 1978.
(4) Chamberlain, J. W. *Theory of Planetary Atmospheres*; Academic: New York, 1978.
(5) *Atmospheric Physics and Chemistry*; Massey, H. S. W., Bates, D. R., Eds.; Academic: New York, 1982.
(6) *Molecular Astrophysics*; Diercksen, G. H. F., Huebner, W., Langhoff, P. W., Eds.; Reidel: Dordrecht, The Netherlands, 1985.
(7) McCartney, E. J. *Absorption and Emission by Atmospheric Gases*; Wiley: New York, 1983; p 9.
(8) Gallagher, J. W.; Brion, C. E.; Samson, J. A. R.; Langhoff, P. W. *J. Chem. Phys. Ref. Data* **1988**, *17*, 9.
(9) Smith, M. E.; Lucchese, R. R.; McKoy, V. *J. Chem. Phys.* **1983**, *79*, 1360.
(10) Brion, C. E.; Hamnett, A. *Adv. Chem. Phys.* **1981**, *45*, 1.
(11) Brion, C. E. *Comments At. Mol. Phys.* **1985**, *16*, 249.
(12) Hatano, Y. *Phys. Rep.* **1999**, *313*, 109.
(13) Hatano, Y. *The Physics of Electronic and Atomic Collisions*; Dube, L. J., Mitchell, J. B. A., McConkey, J. W., Brion, C. E., Eds.; AIP Press: New York, 1995.
(14) Eparvier, F. G.; Barth, C. A. *J. Geophys. Res.* **1992**, *97*, 13723.
(15) Wayne, R. P. *Chemistry of Atmospheres*, 3rd ed.; Oxford University Press: Oxford, England, 2000.
(16) Shematovich, V. I.; Bisikalo, D. V. *J. Geophys. Res.* **1994**, *29*, 23217.
(17) Hermann, M. R.; Bauschlicher, C. W.; Huo, W. M.; Langhoff, S. R.; Langhoff, P. W. *Chem. Phys.* **1986**, *109*, 1.
(18) Martín, I.; Lavín, C.; Velasco, A. M.; Martín M. O.; Karwowski, J.; Diercksen, G. H. F. *Chem. Phys.* **1996**, *202*, 307.
(19) Martín, I.; Lavín, C.; Karwowski, J. *Chem. Phys. Lett.* **1996**, *255*, 89.
(20) Velasco, A. M.; Martín, I.; Lavín, C. *Chem. Phys. Lett.* **1997**, *264*, 579.
(21) Martín, I.; Velasco, A. M.; Lavín; C. *Adv. Quantum Chem.* **2001**, *39*, 145.
(22) Martín, I.; Velasco, A. M.; Lavín, C.; Olalla, E.; Bustos, E. *Int. J. Quantum Chem.* **2001**, *85*, 345.
(23) Bustos, E.; Velasco, A. M.; Martín, I.; Lavín, C. *J. Phys. Chem. A* **2002**, *106*, 35.
(24) Erman, P.; Karawajczyk, A.; Rachlew-Källen, E.; Strömholm, C. *J. Chem. Phys.* **1995**, *102*, 3064.
(25) Edqvist, O.; Asbrink, L.; Lindholm, E. *Z. Naturforsch.* **1971**, *26*, 1407.
(26) Iida, Y.; Carnovale, F.; Daviel, S.; Brion, C. E. *Chem. Phys.* **1986**, *105*, 211.
(27) Southworth, S. H.; Trueslade, C. M.; Cobrin, P. H.; Lindle, D. W.; Brewer, W. D.; Shirley, D. A. *J. Chem. Phys.* **1982**, *76*, 143.
(28) Brunger, M. J.; Campbell, L.; Cartwright, D. C.; Middleton, A. G.; Mojarrabi, B.; Teubner, P. J. O. *J. Phys. B: At. Mol. Opt. Phys.* **2000**, *33*, 783.
(29) Barrientos, C.; Martín, I. *Can. J. Phys.* **1988**, *66*, 29 and references therein.
(30) Mulliken, R. S. *J. Am. Chem. Soc.* **1964**, *86*, 3183.
(31) Hermann, M. R.; Langhoff, S. R.; Gil, T. J.; Langhoff, P. W. *Chem. Phys Lett.* **1986**, *125*, 336.
(32) Martín, I.; Simons, G. *J. Chem. Phys.* **1975**, *62*, 4799.
(33) Sander, M.; Chewter, L. A.; Muller-Dethlefs, K.; Schlag, E. W. *Phys. Rev. A* **1987**, *36*, 4546.
(34) Rabadán, I.; Tennyson, J. *J. Phys. B: At. Mol. Opt. Phys.* **1996**, *29*, 3747.

(35) Edlèn, B. *Handbuch der Physik*; Springer-Verlag: Berlin, 1964; Vol. 27.
(36) Velasco, A. M.; Bustos, E.;.Martín, I.; Lavín, C. *J. Phys. Chem. A* **2002**, *106*, 6401.
(37) Jungen, C. *J. Chem. Phys*. **1970**, *53*, 4168.
(38) Johns, J. W. C. *Mol. Spectrosc*. **1974**, *2*, 513.
(39) Kaufmann, K. *J. Phys. B: At. Mol. Opt. Phys.* **1991**, *24*, 2277.
(40) Huber, K. P.; Miescher, E. *Helv. Phys. Acta* **1968**, *36*, 987.
(41) Suter, R. *Can. J. Phys.* **1969**, *47*, 881.
(42) Dressler, K.; Miescher E. *Astrophys. J*. **1965**, *141*, 1266.
(43) Fano, U.; Cooper, J. W. *Rev. Mod. Phys.* **1968**, *40*, 441.
(44) Parkinson, W. H.; Reeves E. M.; Tomkins, F. S. *J. Phys. A: Math. Gen.* **1976**, *9*, 157.
(45) Lin, C. D. *Astrophys. J.* **1974**, *187*, 385.